



## COPY RIGHT

**2018 IJIEMR.** Personal use of this material is permitted. Permission from IJIEMR must be obtained for all other uses, in any current or future media, including reprinting/republishing this material for advertising or promotional purposes, creating new collective works, for resale or redistribution to servers or lists, or reuse of any copyrighted component of this work in other works. No Reprint should be done to this paper, all copy right is authenticated to Paper Authors

IJIEMR Transactions, online available on 26<sup>th</sup> January 2018. Link :

<http://www.ijiemr.org/downloads.php?vol=Volume-7&issue=ISSUE-01>

Title: MLI based Photovoltaic systems for single phase grid connected system.

Volume 07, Issue 01, Page No: 219 – 229.

Paper Authors

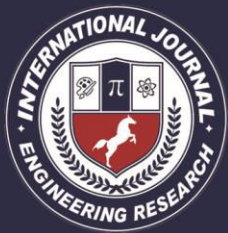
\* **BIRELLA.ANURADHA, GALLA.NAGARAJU.**

\* Dept of EEE, Narasaraopet Engineering College.



USE THIS BARCODE TO ACCESS YOUR ONLINE PAPER

To Secure Your Paper As Per **UGC Guidelines** We Are Providing A Electronic Bar Code



## MLI BASED PHOTOVOLTAIC SYSTEMS FOR SINGLE PHASE GRID CONNECTED SYSTEM

\*BIRELLA.ANURADHA, \*\* GALLA.NAGARAJU

\*PG Scholar, Department of Electrical & Electronics Engineering, Narasaraopet Engineering College, Narasaraopet; Guntur (Dt); Andhrapradesh, India.

\*\*Assistant Professor, Department of Electrical & Electronics Engineering, Narasaraopet Engineering College, Narasaraopet; Guntur (Dt); Andhrapradesh, India.

[anuradha641@gmail.com](mailto:anuradha641@gmail.com)

[nagaraj204@gmail.com](mailto:nagaraj204@gmail.com)

### ABSTRACT:

In this project MLI based Photovoltaic systems for single phase grid is proposed. Photovoltaic systems require interfacing power converters between the PV arrays and the grid. These power converters are used for two major tasks. First, is to inject a sinusoidal current in to the grid. And second is to reduce the harmonics content in the grid injected voltage and current. Normally there are two power converters. The first one is a DC/DC power converter that is used to operate the PV arrays at the maximum power point. The other one is a DC/AC power converter to interconnect the photovoltaic system to the grid. Multilevel converters enable the output voltage to increase without increasing the voltage rating of the switching devices, so that they offer the direct connection of renewable energy systems to the grid voltage without using the expensive and bulky transformers. This project proposes photovoltaic system with a multilevel inverter connected to a grid for getting better performance which is shown by using MATLAB/SIMULINK model.

**Keywords**— photovoltaic energy; grid-connected; voltage oriented control; single phase; inverter.

### 1. INTRODUCTION

Addressing the ever increasing global demand on reliable and sustainable electricity has become a main concern of electricity sector. At the moment, fossil fuel power plants are the backbone of world's electricity generation system. On the other hand, they are recognized as a major cause for the environmental pollutions. Today, millions are willing to enjoy the benefits of improved lifestyle and environment with much more electricity generated from the renewable energy sources. In 2010, renewable energies accounted for 16.6% of the world's primary energy demand, while a share up to 50% worldwide is feasible by 2040, according to a report published by the European Renewable Energy Council (EREC) together with its member associations (EPIA, ESHA, ESTIF, EUBIA, EUREC Agency, EWEA, AEBIOM and EGEC). Along with ambitious plans to increase the share of renewable energies in developed countries, such as EU 2020 political renewable energy goal,

and progresses in renewable energy utilization in developing and newly industrializing countries, small-scale electricity generation systems, such as small hydro turbines, roof mounted photovoltaic and wind generation systems, and commercially available fuel cells are being widely utilized at the distribution level. The general structure of a small-scale renewable energy source, which is usually interfaced with the single-phase grid through a stage of power electronic devices, is depicted. The source side power conversion system extracts the maximum electricity from the available renewable input power and its topology and control strategy highly depends on the type of the renewable energy source.

The focus of this paper is on the grid-side converter. The main objective of the grid-side converter is to control the power flow between the ac system and the dc link powered from the renewable resources. The single-phase voltage

source converter (VSC) is the best solution for interfacing with a single-phase grid. It offers several advantages such as bidirectional power flow capability and low distortions at the ac side current and the dc side voltage. Another promising feature is that it can independently control the active and reactive power exchanged with the ac network; therefore, it can improve the voltage profile, and is able to operate in weak ac systems. These advantages make the single-phase VSC a successful solution for grid integration of small-scale renewable energy sources. To regulate the power exchange with the single-phase grid, and at the same time, reduce the harmonic distortions in the ac current, different current control structures have already been proposed, such as current hysteresis control (CHC), voltage oriented control (VOC), and proportional-resonant (PR) based control, which all have their own pros and cons.

This paper gives an overview of the main characteristics of these control strategies. The paper also includes a discussion of some implementation aspects such as the fictitious signal generation and the single-phase grid synchronization techniques. Then, through extensive simulations a comparative study of the presented control strategies is presented and discussed. The simulations are supported by experiments.

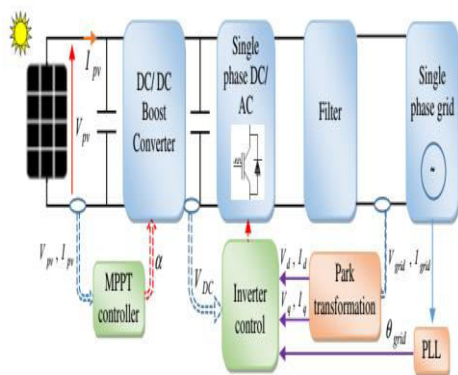


Fig.1 Scheme of the proposed photovoltaic system connected to a single-phase grid utility

## (II) SYSTEM MODELLING

To have an efficient control strategy, models for the system components are needed. Hence, in this section, the system components models are presented.

### A. Photovoltaic panels

A one-diode based non-linear model is used to model the photovoltaic panels, using an ideality factor to describe the diode's performance [8, 9]. The model uses the radiation  $G(t)$ , the ambient temperature  $T_a(t)$  at the panel surface, and the panel parameters to evaluate the photovoltaic current  $I_c(t)$  [10]. The adopted model is described by (1)-(6) [10, 11]:

$$\frac{a}{V_c(t) + R_s i_c(t)} \exp(-1) - \left( \frac{V_c(t) + R_s i_c(t)}{R_p} \right) \quad (1)$$

$$I_c = I_{ph}(t) - I_r(t)$$

$$I_{ph}(t) = \frac{G(t)}{G_{ref}} I_{sc}(t) \quad (2)$$

$$I_{sc}(t) = I_{sc} \left( 1 + a(T_a(t) - T_{ref}) \right) \quad (3)$$

$$I_r(t) = I_{ref} \left( \frac{T_a(t)}{T_{ref}} \right)^{\frac{3}{n}} \exp\left( \frac{-qV_c}{nK_B} \left( \frac{1}{T_a(t)} - \frac{1}{T_{ref}} \right) \right) \quad (4)$$

$$\frac{qV_c}{nK_B T_{ref}} - 1 \quad (5)$$

$$r = I$$

where:

$T_a(t)$ : the ambient temperature at the panel surface (K),

$G(t)$ : the solar radiance at the panel surface ( $W/m^2$ ),

$I_c(t)t$ : the estimated photovoltaic cell current (A),

$I_{ph}(t)t$ : the generated photo-current at  $G$  (A),

$I_r(t)$ : the reverse saturation current at  $T_a$  (A),

$V_c(t)$ : the open circuit voltage of the photovoltaic cell (V),

$R_s$ : the serial resistance of the photovoltaic module ( $\Omega$ ),

$V_{t-T_a}$ : the thermal potential at the ambient temperature (V),

$R_p$ : the parallel resistance of the photovoltaic module ( $\Omega$ ),

$G_{ref}$ : the solar radiation at reference conditions ( $W/m^2$ ),

$I_{sc}(t)$ : the short circuit current for  $T_a$  (A),

$I_{sc}^{ref}$ : the short circuit current per cell at the

reference temperature  $T_{ref}(A)$ ,

$a$ : the temperature coefficient for the short circuit current ( $K^{-1}$ ),

$I_r^{ref}$ : the reverse saturation current for  $T_{ref}(A)$ ,

$n$ : the quality factor,

$q$ : the electron charge (C),

$V_g$ : the Gap energy (e.V),

$K_B$ : the Boltzmann coefficient (J/K),

$V_c^{ref}$ : the open circuit voltage per cell at  $T_{ref}(V)$ .

The photovoltaic power  $P_{pv}$  generated by the panel is then described as follows [11- 13]:

$$P_{pv}(t) = n_s n_p V_c(t) \frac{a}{V_c(t) + R_s I_c(t)} \frac{\exp(-1)}{V_c(t) + R_s I_c(t)} \frac{1}{R_p} (I_{ph}(t) - I_r(t)) \quad (6)$$

where:

$n_s$ : the number of serial photovoltaic cells,  
 $n_p$ : the number of parallel photovoltaic modules.

**B. Incremental conductance for MPPT** Thanks to its efficiency, the incremental conductance algorithm for MPPT is used to track the Maximum Power Point (MPP) of the photovoltaic panels, and generate the control signal for the boost converter [14] (Fig. 2). In fact, this method uses the current ripple in the chopper output  $I_{pv}$  to maximize the panel power  $P_{pv}$  using the relation between the current and voltage continuously identified online [15, 16].

Indeed, the algorithm tests the actual conductance  $-I_{pv}/V_{pv}$  and the incremental conductance  $dI_{pv}/dV_{pv}$  as follows [13, 17, 18]: Thus, the duty cycle  $\alpha$ , used to generate the PWM signal for the MOSFET switching, is calculated using (10) [20]:

$$\frac{V_{dc}}{V_{pv}} = \frac{1}{1-\alpha} \quad (10)$$

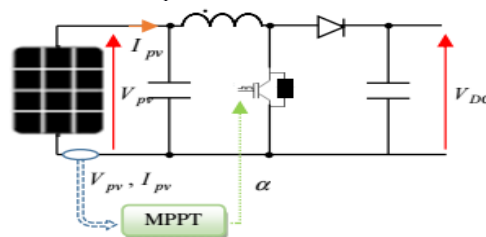
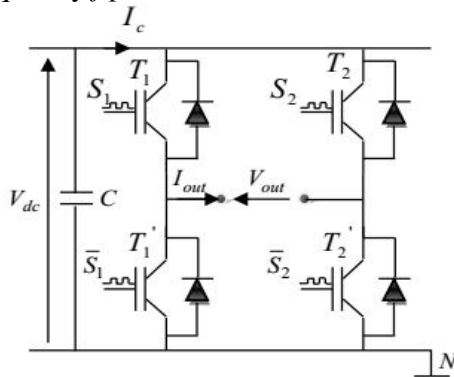


Fig.2 Control principle of the boost converter for the MPPT

### C. Single-phase DC/AC inverter

A full bridge inverter is used to convert DC voltage and current to AC voltage and current (Fig. 3). The inverter is controlled by a PWM

signal, which allows the control signals  $S1$  and  $S2$  to be deduced. In fact, this modulation obtained by comparing referential sinusoidal signals called modulating waves (characterized by the frequency  $f_r$  and the amplitude  $V_r$ ) with a triangular signal (called carrier wave, characterized by a frequency  $f_p \ll f_r$ , and the amplitude  $V_p$ ) [21]. The first leg is controlled by a signal  $V_{modulation}$ , while the second leg is controlled by  $-V_{modulation}$ . When the two signals take the same value, the IGBTs change the state, so PWM signals are generated, with the frequency  $f_p$  [21]



**Fig.3 Single-phase full bridge inverter**

The switches  $T1, T1', T2$  and  $T2'$  are connected as follows:

- If  $V_{modulation} > V_{carrier}$ , then  $T1$  is **on**
- If  $V_{modulation} < -V_{carrier}$ , then  $T1'$  is **on**
- If  $-V_{modulation} > V_{carrier}$ , then  $T2$  is **on**.
- If  $-V_{modulation} < -V_{carrier}$ , then  $T2'$  is **on**.

Hence, the inverter output voltage is evaluated by (Fig.4):

$$V_{out}(t) = V_{AN}(t) - V_{BN}(t) \quad (11)$$

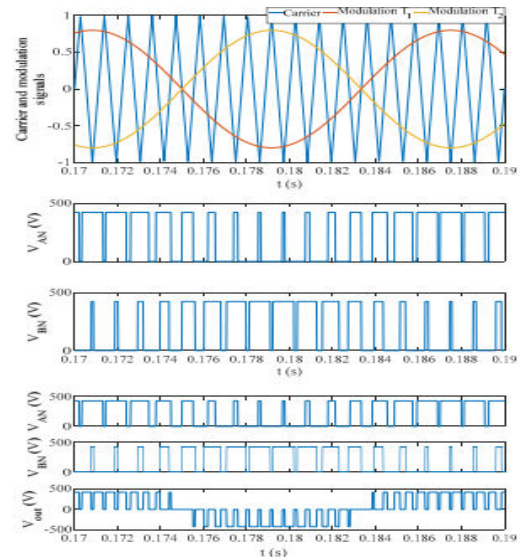


**Fig.4 PWM based control for single-phase inverter**

### (III) CONTROL STRATEGY PRINCIPLE

#### A. Inverter Converter

The voltage-oriented control or VOC regulates the active and reactive currents by orienting the current vector with respect to the line voltage vector. In fact, VOC is performed in the direct-quadrature (d, q) synchronous reference frame, where the error between the direct ( $I_d$ ) and quadrature ( $I_q$ ) components of the AC current and their reference values are fed to the PI controllers [22]. Then, the regulator PI generates the reference voltage for the converter, which is applied to the AC converter using a PWM modulator. Hence, all electrical signals are transformed to the synchronous reference frame, where quantities are DC and, as a consequence, the zero steady-state error is ensured by using a conventional proportional-integral (PI) controller (Fig. 5).

To perform the VOC, two orthogonal signals are needed. As a consequence, a fictitious phase must be generated. To create a two phase system from a single phase signal, the transport delay method is used here [23].

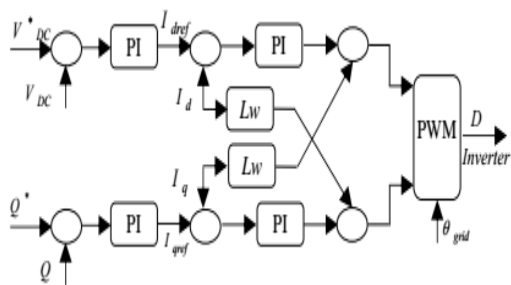


Fig.5 Simplified block-diagram of VOC based control of single-phase grid-tie converters

### B. Fictitious phase generation

The single-phase circuit has one phase conductor with a neutral return. In order to extend the synchronous (d, q) reference frame control strategies to single-phase systems, two orthogonal signals are needed. Hence, a second fictitious phase should be properly generated, to model a single-phase circuit as an equivalent virtual two-phase circuit. In the literature, there are several successful works for generating the fictitious phase including the transport delay [24], Hilbert transformation [25, 26], all-pass filter [27], and SOGI [28] methods. In this paper, the transport delay method is used to generate the fictitious phase, since it is simple and can be implemented by digital controllers without the need for tuning any parameters [28] (Fig. 6). Indeed, a phase shift of  $90^\circ$  with respect to the fundamental frequency of the input signal is realized through the use of a first-in-first-out memory, with the delay adjusted to one fourth the number of total samples of a cycle of the fundamental frequency [28].

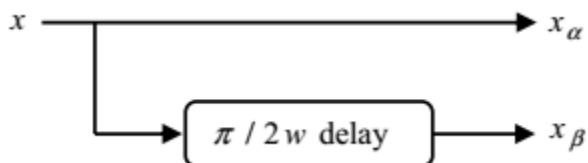


Fig.6 Transport delay method to generate the fictitious phase signal

### C. Single phase synchronization

Among several synchronization techniques, the phase locked loops (PLLs) are the most used technique for synchronization, thanks to its

simplicity, robustness, and effectiveness. In fact, the PLL is a closed loop feedback control system, which synchronizes its output signal in phase, as well as in frequency, with the fundamental component of the grid voltage. Among various techniques, currently, the synchronous reference frame PLL (SRF-PLL) is the most common technique used for single phase grid synchronization [28] (Fig. 7).

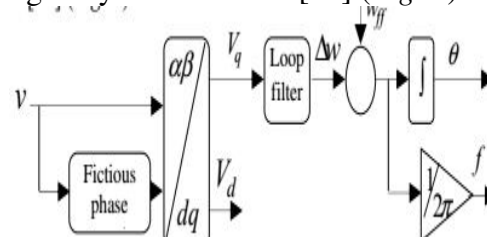


Fig.7 Control strategy for the grid-connected photovoltaic panel

### D. Current control loop

The current control loops are used to control the direct and quadrature grid currents,  $I_d$  and  $I_q$ , respectively. In fact, these components are compared with the respective reference component  $I_{dref}$  and  $I_{qref}$ , and the resultant errors are used by PI regulator to generate the inverter control signal, which allows the AC signals to be generated, following the grid characteristics (frequency and phase) [23].

Indeed, the direct current component controls the grid active power flow, while the q component is used here to regulate the reactive power flow. Hence, a voltage loop, which regulates the mean and measured voltages at the Boost output, is used to generate the reference direct current  $I_{dref}$  (Fig. 5). While, the quadrature current reference  $I_{qref}$  is generated by the grid phase control loop (Fig. 8).

The DC bus voltage is maintained constant by a voltage loop, which allows the continuous active power flow between the PV array and the grid, to be maintained. Thus, a PI regulator uses the difference between the reference and measured signals of the DC voltage to generate the reference signal of the direct current  $I_{dref}$  (12) [23]:

$$C_{DC} \frac{dV_{DC}}{dt} = \frac{P_{pv} - P_{grid}}{V_{DC}} \quad (12)$$

### E. Reactive power control

The reactive power is controlled by the power coefficient control. In fact, the reactive power control is ensured by generating the reference signal of the reactive current component  $I_{qref}$ , thanks to a PI regulator. Fig. 8 shows the simplified block diagram of the reactive power control loop.

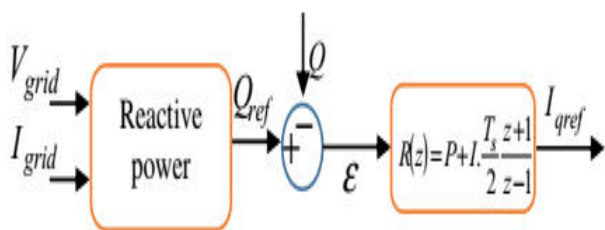


Fig.8 Block diagram of the reactive power control loop

## (IV) FIVE LEVEL INVERTER

### Five Level Inverter for Grid Connected Application

A DC-AC inverter is employed that generate a sinusoidal current compiled with international standard to be either injected into grid or to fed local and remote load. A five-level bidirectional converter is developed and applied for PV integration to the power grid. The converter is configured by two dc capacitors, a three converter part, an unfolding bridge and a filter. It will operate in two modes, rectifier mode and inverter mode. During the start-up, the grid acts as the source and the 5works in rectifier mode.

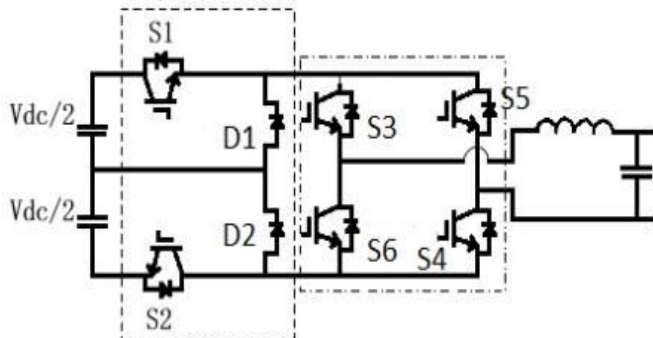
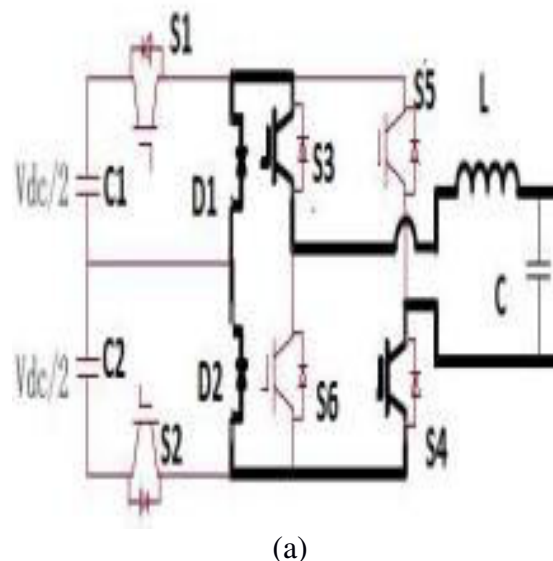


Figure 9: Five level inverter

After the PV optimizer stage starts, the converter will automatically work in inverter mode and generate an output voltage with five levels. In both modes, only two high frequency switches will operate and the unfolding bridge will work at grid frequency. The Five level inverter is developed from this bidirectional converter, considering only the inverter mode of operation. With the control strategy, the dc link capacitor voltages are balanced and therefore only one source is required compared to other multilevel topology and the number of switches is reduced compared to the diode clamped, flying capacitor and cascade H-bridge 5 level inverters with the same voltage levels.

### Operating Modes

The operation of the five-level converter can be divided into rectifier and inverter mode. The converter operates mainly in inverter mode as a grid-tie inverter. In this mode, only S1 and S2 operate at high frequency. The switches S3 and S4 will be ON only during positive half cycle and S5 and S6 will be ON only during the negative half cycle. The inverter mode could be further divided into eight modes.



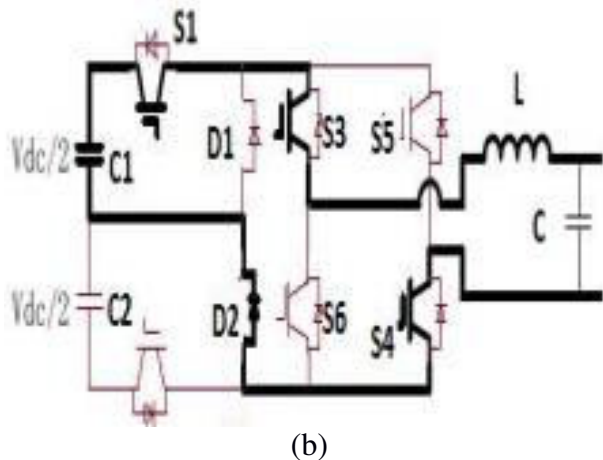


Fig 10. Modes of Operation of 5 level inverter  
(a) Mode 1 (b) Mode 2

### a. INV Mode 1

Figure 10 (a) shows operation circuit of INV Mode 1. Both S1 and S2 are turned off. The current of the filter inductor flows through S3, S4 and the two body diodes of D1 and D2. The inverter output is 0.

### b. INV Mode 2

Figure 10 (b) shows operation circuit of INV Mode 2. S1 is turned on and S2 is turned off. DC capacitor C1 is discharged through S1, S3, filter inductor, S4 and the body diode of S2 to form a loop. The inverter output is  $V_{dc}/2$ .

### c. INV Mode 3

Figure 11(a) shows operation circuit of INV Mode 3. Both S1 and S2 are turned on. DC capacitors C1 and C2 are both discharged through S1, S3, filter inductor, S4 and S2. The inverter output is  $V_{dc}$ .

### d. INV Mode 4

Figure 11(b) shows operation circuit of INV Mode 4. S1 is turned off and S2 is turned on. DC capacitor C2 is discharged through the diode of D1, S3, filter inductor, S4 and S2 to form a loop. The inverter output is  $V_{dc}/2$ .

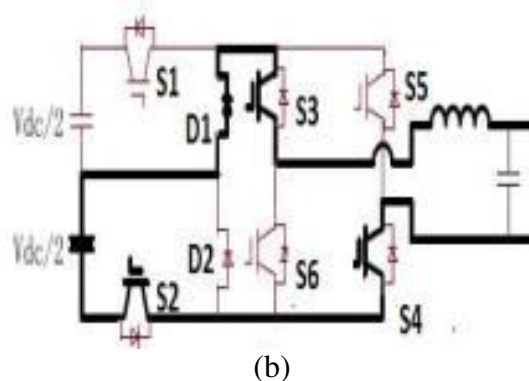
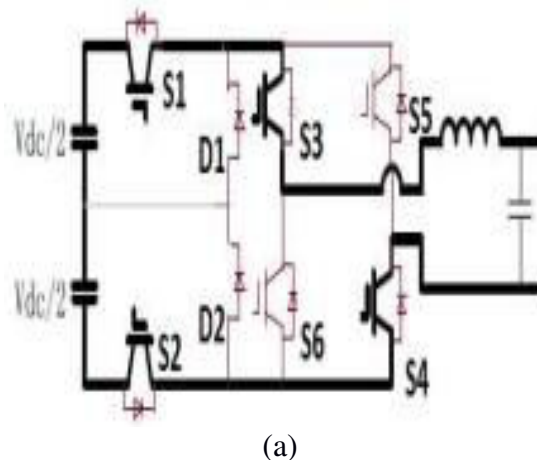


Figure 11. Modes of operation (a) Mode 3 (b) Mode 4

The operations of the converter under INV mode 5-8 are similar to that under INV mode 1-4. The inverter output is 0,  $V_{dc}/2$  and  $V_{dc}$ , respectively. The inverter therefore, can have a five-level voltage output, which is  $V_{dc}$ ,  $V_{dc}/2$ , 0,  $V_{dc}/2$  and  $V_{dc}$ . The PWM strategy is used in the control section which helps balance the DC link capacitors. In PWM strategy, S1 and S2 will be turned on, turned off, turned on alternatively or turned off alternatively. The voltage balance issue is important for multi-level inverter. If the capacitor voltages are not balanced, the output voltage may become unsymmetrical and result in high harmonics in load current. No shoot through issues for the two high frequency switches, and no dead zone needed, which reduces the harmonics of the output and simplifies the control.



## (V) SIMULATION RESULTS

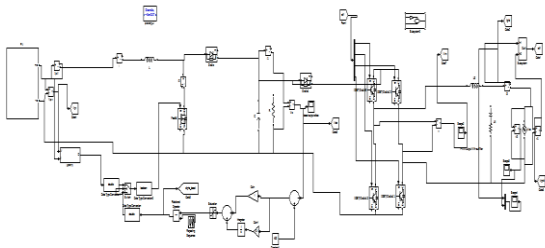
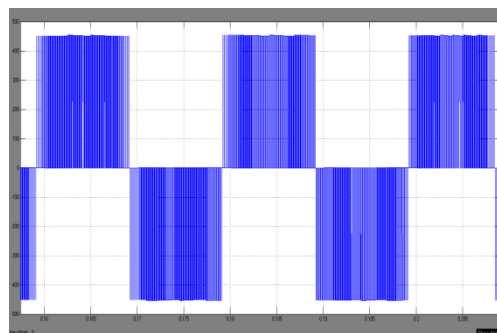


Fig 12 Simulink diagram of proposed concept



(a) Inverter voltage

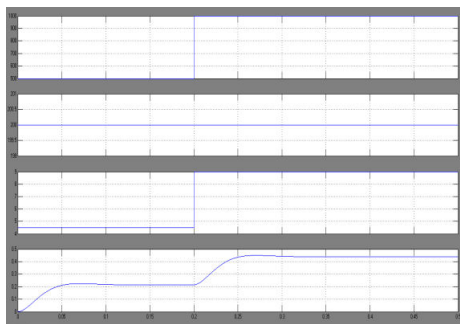
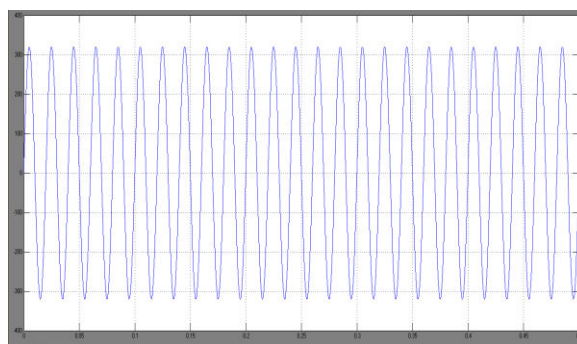


Fig.13 Photovoltaic panel characteristics



(b) Grid voltage

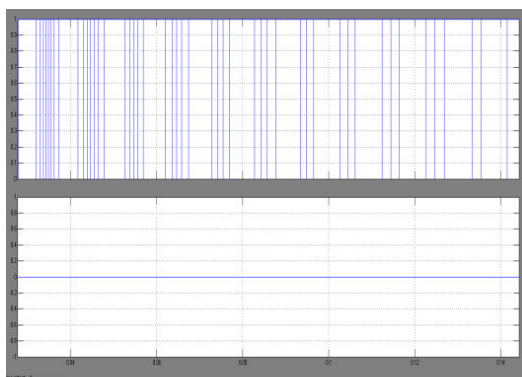
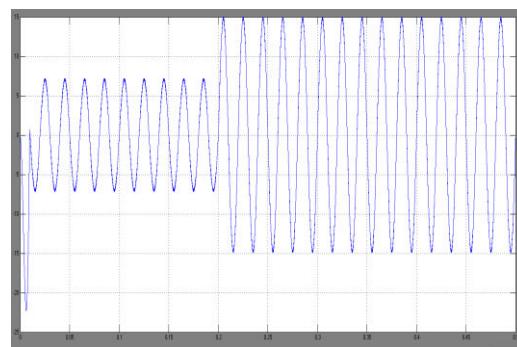


Fig.14 MPPT incremental conductance results



(c) grid current

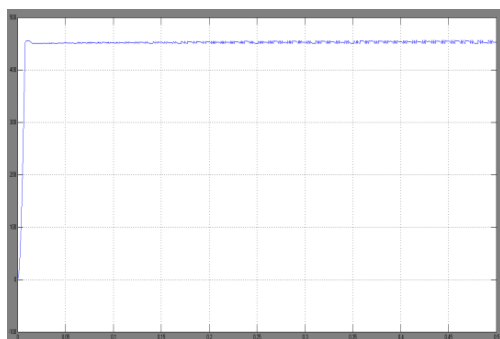
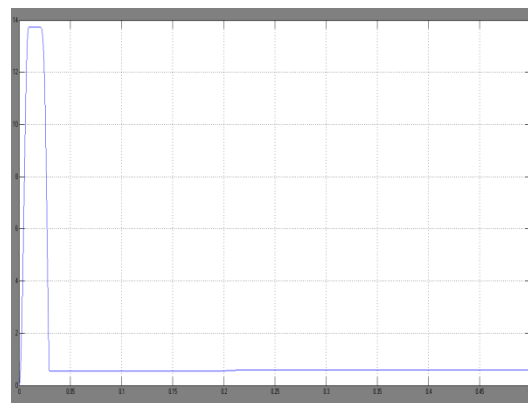


Fig.15 Output voltage at the boost converter terminals



(d) Modulation Index

Fig.16 Inverter control results

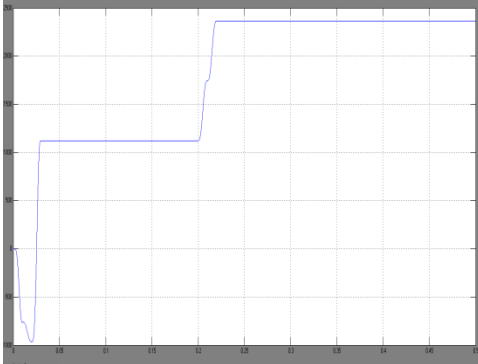


Fig.17 Active power control results

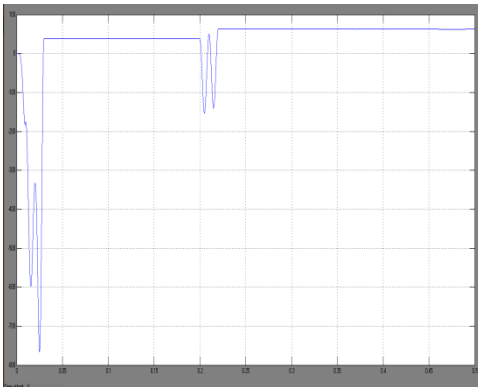


Fig.18 Reactive power control results

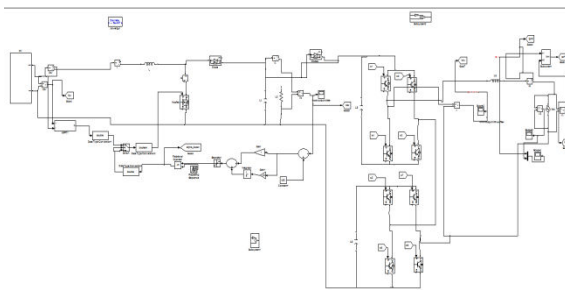


Fig 19 Simulink diagram five level converter

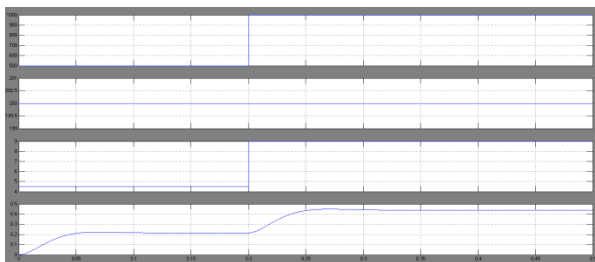


Fig.20 Photovoltaic panel characteristics

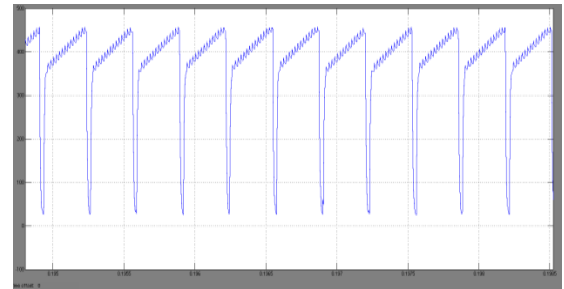


Fig.21 Output voltage at the boost converter terminals

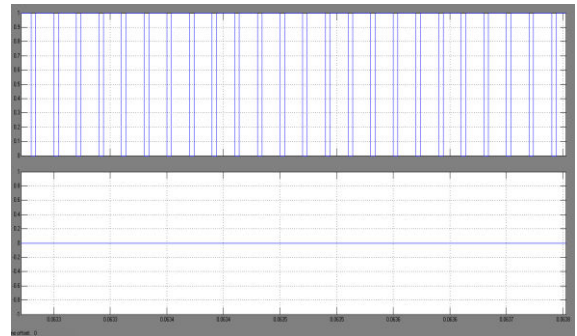
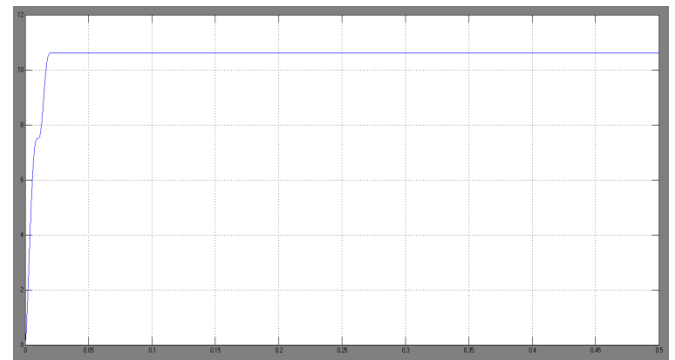
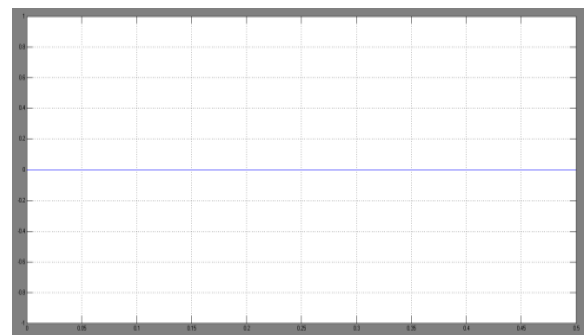


Fig.22 MPPT incremental conductance results

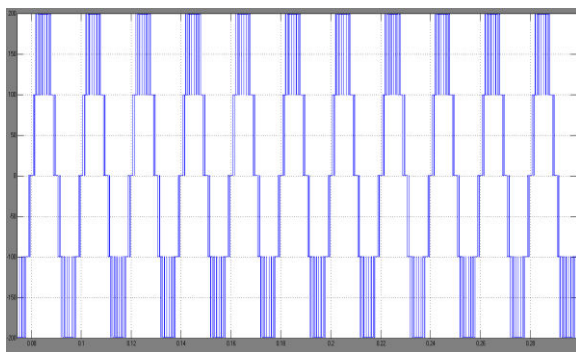


(a) direct axis  $I_d$  vs time (t)



(b) quadrature axis ( $i_q$ ) vs time

Fig.23 Direct and quadrature currents characteristics



(a) Inverter voltage

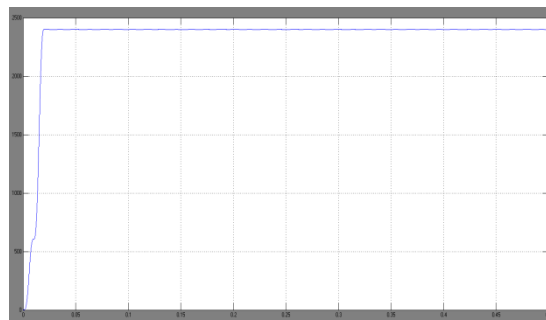
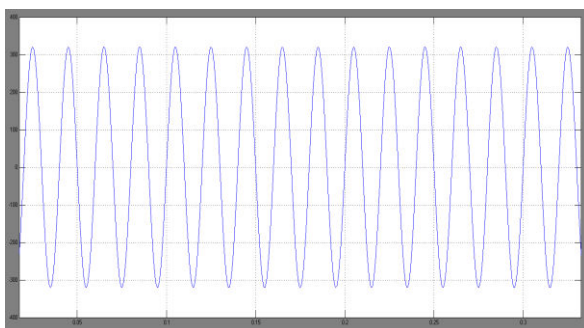


Fig.25 Active power control results



(b) Grid voltage vgrid

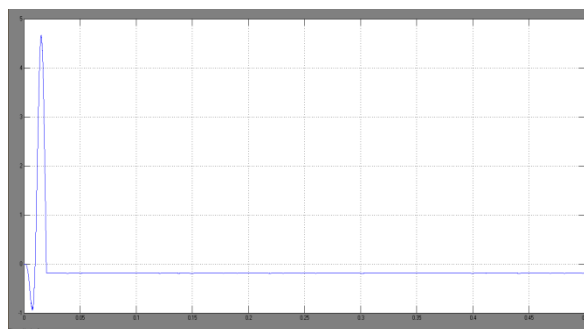
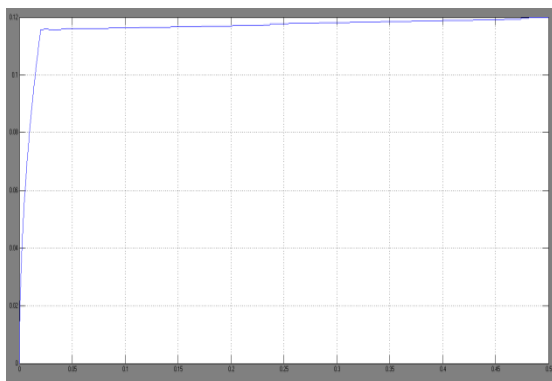


Fig.26 Reactive power control results



(c) grid current Igrid



(d) Modulation index vs time  
Fig.24 Inverter control results

## (VI) CONCLUSION

In this paper, a single-phase inverter control is studied in depth. The control strategy uses the voltage oriented control to control the active and passive powers. Following the above conducted studies, one can conclude that VOC presents good results in controlling a single-phase grid connected inverter. In a future work, the authors will present the effect of intermittent changes for the climatic parameters in the performance of single-phase grid connected inverters.

## REFERENCES

- [1] L. Zhang, N. Gari, and L. V. Hmurcik. "Energy management in a microgrid with distributed energy resources", Energy Conversion and Management, vol. 78, pp. 297-305, 2014.
- [2] K.S. Reddy, M. Kumar, T.K. Mallick, H. Sharon, and S. Lokeswaran. "A review of Integration, Control, Communication and

Metering (ICCM) of renewable energy based smart grid”, *Renewable and Sustainable Energy Reviews*, vol. 38, pp. 180-192, 2014.

[3] J. Urbanetz, P. Braun, and R. R  ther, “Power quality analysis of grid connected solar photovoltaic generators in Brazil”, *Energy Conversion and Management*, vol. 64, pp. 8-14, 2012.

[4] B. G  kay, “A remote islanding detection and control strategy for photovoltaic-based distributed generation systems”, *Energy Conversion and Management*, vol. 96, pp. 228-241, 2015.

[5] B. Bahrani, A. Rufer, S. Kenzelmann, and L. Lopes, “Vector control of single-phase voltage-source converters based on fictive-axis emulation”, *IEEE Transactions on Industrial Applications*, vol. 47, pp. 831-40, 2011.

[6] M. Amin, and O. Mohammed, “Vector oriented control of voltage source PWM inverter as a dynamic VAR compensator for wind energy conversion system connected to utility grid”, *Applied power electronics conference and exposition (APEC)*, pp. 1640-1650, 2010.

[7] S. Samerchur, S. Premrudeepreechacharn, Y. Kumsuwun, and k. Higuchi, “Power control of single-phase voltage source inverter for grid-connected photovoltaic systems”, *Power systems conference and exposition (PSCE)*, pp 1-6, 2011.

[8] C. F. M. Toledo, L. Oliveira, and P. M. Frana. “Global optimization using a genetic algorithm with hierarchically structured population”, *Journal of Computational and Applied Mathematics*, vol. 261, pp. 341- 351, 2014.

[9] A. Mellit, M. Benghanem, A. Hadj Arab, and a. Guessoum, “Modelling of sizing the photovoltaic system parameters using artificial neural network”, *IEEE Conference on Control Applications*, pp. 353-357, 2003.

[10]H. Yang, Z. Hongxing, L.L. Zou, and Z. Fang, “Optimal sizing method for stand-alone hybrid solar-wind system with LPSP

technology by using genetic algorithm”, *Solar Energy*, vol. 82, pp. 354-367, 2008.

[11]T. Khatib, M. Azah, K. Sopian, and M. Mahmoud, “A new approach for optimal sizing of standalone photovoltaic systems”, *International Journal of Photo Energy*, 2012.

[12]I. Yahyaoui. “Sizing and energy management of photovoltaic water pumping”, *International Thesis presented at the University of Valladolid, Spain*, 2015.

[13]S. A. Klein, and W. A. Beckman, “Loss-of-load probabilities for standalone photovoltaic systems”, *Solar Energy*, vol. 39, pp. 499-512, 1987.

[14]D. P. Hohm, and M. E. Ropp, “Comparative study of maximum power point tracking algorithms”, *Progress in photovoltaics: Research and Applications*, vol. 11, pp. 47-62, 2000.

[15]I. Yahyaoui, M, Chaabene, and F, Tadeo, “Evaluation of Maximum Power Point Tracking algorithm for off-grid photovoltaic pumping”, *Sustainable Cities and Society*, 2015.

[16] Li, Shaowu, “A maximum power point tracking method with variable weather parameters based on input resistance for photovoltaic system”, *Energy Conversion and Management*, vol. 106 (2015): 290-299.

[17]Single stage three level grid interactive MPPT inverter for PV systems Saban Ozdemira, , Necmi Altinb, , , Ibrahim Sefa Volume. 80, April 2014, Pages 561-572